ARTICLE / INVESTIGACIÓN

Synthesis, characterization, biological studies and DFT study of Schiff Bases and their complexes derived from aromatic diamine compounds with cobalt (II)

Abduljleel Mohammed Abduljleel, Jassim Mohammed Saleh Alshawi, kawkab Ali Hussein*, Sadiq M-H. Ismael

DOI. 10.21931/RB/2023.08.01.61

Department of Chemistry, College of Education for Pure Sciences, University of Basrah, Basrah, 61004 Iraq.
Corresponding author: kawkab.ali@uobasrah.edu.iq.

Abstract: Based on vanillin and diamine compounds (ortho phenylene diamine, meta phenylene diamine, 3,4- diamine toluene), derivation of two new Schiff base ligands (L^1 and L^2) was done, after which synthesis and treatment with Co (II) chloride was performed at a metal-to-ligand ratio of 1:1 to get two new complexes, i.e. $[CoL^3(H_2O)_2]Cl_2$ and $[CoL^1(H_2O)_2]Cl_2$. These complexes and ligands were characterized by employing NMR, IR, atomic absorption, UV visible absorption, molecular weight determination, molar conductance, and magnetic measurement techniques. As per the data, the ligands were found to be bidentate ligands that were linked to two azomethine nitrogen sites. It was suggested that these complexes were paramagnetic electrolyte compounds that possessed coordination number four. Screening of the ligands and metal complexes was done to assess their antimicrobial activities against gram-negative and gram-positive bacteria, which was found to show biological activity. Calculations using quantum chemistry were done to examine the molecule geometry. The investigation includes several quantum chemical characteristics derived from frontier molecular orbitals.

Key words: Schiff bases, transition metal complexes, vanillin, diamine aromatic compounds, antibacterial activity, DFT study.

Introduction

The general structure of Schiff bases includes R-CH=N-Ar, wherein Ar and R represent the aromatic and aliphatic groups due to the condensation of primary amines with ketones or aldehydes[1]. These can be characterized based on the (-N=CH-) groups, which include biological characteristics like antimicrobial[2], antifungal[3] and anticancer activities[4]. Schiff bases derived based on diamines and aldehydes have one of the most critical synthetic ligand systems for asymmetric catalysis. They are considered significant for a wide variety of progress metal catalysis responses, including epoxidation of ole-fins[5], lactide polymerisation[6], and the opening of the asymmetric rings of epoxides[7]. The chelating Schiff base ligands derived based on different carbonyl compounds, and diamines include a highly notable class of compounds with numerous applications in synthetic[8], catalytic clinical[9], analytical[10], and biochemical[11] processes. Previous studies have shown that enhancement of the coordinating potential of diamine compounds like meta phenylene diamine happens when they are condensed with different carbonyl compounds. However, the literature review did not show any studies or research work conducted regarding the transition metal complexes of Schiff bases that have been derived from vanillin and certain diamines. The current research focuses on preparing Schiff bases based on the condensation of vanillin along with certain aromatic diamines and synthesizing their complexes with cobalt (II) ions. These Schiff bases and complexes have been identified based on 1HNMR, 13CNMR, UV/visible and IR, and atomic absorption techniques. This focus also examined these complexes' conductivity, antibacterial activities, and magnetic characteristics. DFT calculations upheld the research findings. The ground state characteristics of the ligand and its complexes were studied by DFT at the B3LYP/6-31+G (d,p) and B3LYP/LANL2DZ, respectively.

Materials and methods

Merck provided all the employed reagents, which have been used without purification. The melting point was determined based on a Thermo Fisher apparatus. An FTIR – 8400 S – Shimadzu spectrometer was employed to record the IR spectra in the 400–4000 cm^{-1} via KBr pellets. An NMR spectrophotometer (Brucker – 500 MHZ) was used to record the 1HNMR spectra of $CDCl_3$, while a Jenway Pcmb conductivity meter was used to measure the conductance in DMF at room temperature. An SPV-725 (Germany) spectrophotometer was used to record the UV visible spectra in THF. An atomic absorption apparatus (Analyst 200 Atomic Absorption Spectrometer) determined the metal-to-ligand molar ratio. The magnetic properties were measured at room temperature by employing Hg [Co (NCS)4] as the calibrant based on the Gouy method.

Results

Synthesis of Schiff Base Ligands add L^1 and L^2

Vanillin (3.041 gm and 20 mmol) was mixed with diamine (10 mmol) in ethanol (50 mL), and a few drops of glacial acetic acid were added. Then reflux mixture for 14 – 20 hrs. According to the TLC examination, the starting materials

Citation: Abduljleel M A, Jassim M S A, kawkab A H and Sadiq M-H I, Synthesis, Characterization and Biological Studies of Schiff Bases and Their Complexes Derived from Aromatic Diamine Compounds with Cobalt (II). Revis Bionatura 2023;8 (1) 61. http://dx.doi.org/10.21931/RB/2023.08.01.61
Received: 15 January 2023 / **Accepted:** 25 February 2023 / **Published:** 15 March 2023
Publisher's Note: Bionatura stays neutral with regard to jurisdictional claims in published maps and institutional affiliations.

were wholly converted into products. Cooling was applied to obtain the crystalline precipitate that was filtered, cleaned through ethanol, and recrystallized with absolute ethanol before drying. The recommended structure of the prepared ligands is shown in Figure (1), while few of the physical characteristics have been presented in Tables (1) and (2).

Synthesis of Co (II) Complexes

The cobalt complexes were all prepared using the next procedure. A Schiff base ligand and a hot methanolic solution of cobalt (II) chloride hexahydrate were combined in a 1:1 molar ratio. The reaction mixture was refluxed in a water bath for a set amount of time. The colored complex precipitated when the reaction mixture was cooled to room temperature. Filtering was done for the complex and then recrystallized, cleaned with methanol, and then vacuum dried. Figure (2) shows the proposed structure relating to the prepared complexes, while Tables (2) and (3) show certain physical characteristics.

Discussion

Chemistry

The reaction of metal salts with Schiff base donor ligands gives symmetrical Schiff base complexes, as shown in Figures (1) and (2). The Schiff base ligands and their synthesized complexes are colored, air-stable when in the solid state, and possess high melting points. These complexes were found to be insoluble in most common organic solvents like acetone, ethanol, methylene chloride and diethyl ether but were found to be readily soluble in DMSO and DMF. Therefore, the reaction proceeded at a molar ratio of 1:1 (L:M), which resulted in the isolation of four-coordinate complexes. The characterization of the prepared compounds (complexes and ligands) pertains to a range of physicochemical techniques, such as 1H-NMR and mass spectroscopy (for ligands) (Table 1), FT-IR (Table 4) and UV-Vis spectroscopy (Table 5) which are listed as a supplementary file. The isolation of nonelectrolyte complexes is indicated based on measuring the conductance of the complexes in the DMSO solution. With regards to the above data, the isolation of complexes was done with the general formulae $[Cr(L)(Cl_2)(H_2O)]_2$ and $[M(L)Cl]_2$ (where M = Co(II)).

IR and Uv Spectra of Ligands and Complexes

Table (4) and Figures (3 - 6) show the IR absorptions of the ligands and their complexes. The change in the C=N stretching frequencies to down frequencies because of the metal–ligand coordination is regarded to be the most signification difference in the IR spectra of the complexes (L^1Co and L^2Co) and ligands (L^1, L^2). In the complexes (L^1Co and L^2Co), the azomethine vibration about the ligands (L^1, L^2) at 1.502 cm^{-1} and 1.627 cm^{-1} shifted to higher frequencies due to back bonding and the decreasing planar characte-

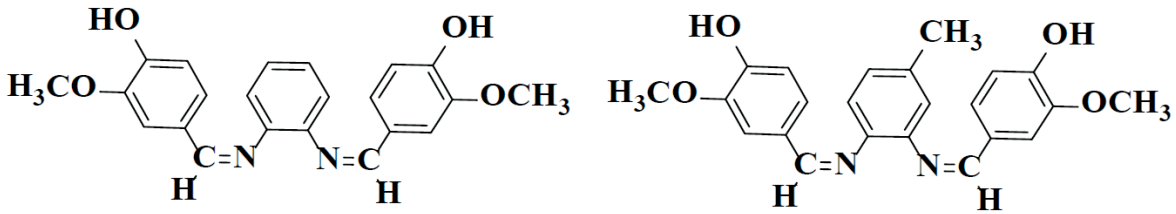

Figure 1. Chemical structure of the prepared Schiff base ligands.

Symbol	Molecular formula	Physical state and colour	Time of reaction (min)	Melting point (°C)	Yield (%)
L^1	$C_{22}H_{20}N_2O_4$	Cream	19	281-283	78
L^2	$C_{23}H_{22}N2O_4$	Yellow	20	257-259	70

: Solubility of prepared Schiff base ligands.

Symbol	ethanol	methanol	acetone	hexane	chlorofor	Petroleum	CH_2Cl_2	benzene	butane	acetonitril	THF	DMF	DMSO	H_2O
L^1	±	±	+	-	+	-	+	+	±	+	+	+	+	-
L^2	±	±	±	-	+	-	+	+	+	±	+	+	+	-

soluble , ± partial soluble , - insoluble.

Table 1. Some physical properties of prepared Schiff base ligands.

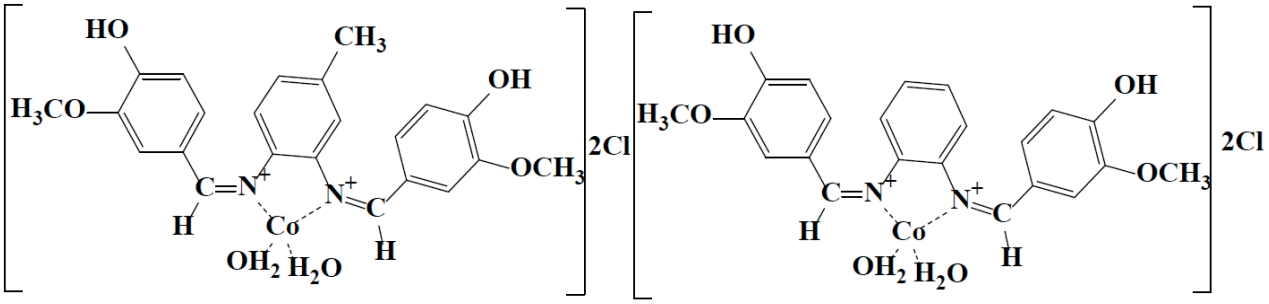

Figure 2. Structure of the prepared complexes.

Symbol	Formula	Physical state and colour	Time of reaction	Melting point (°C)	Yield (%)
L^1Co	$[Co(L^1)(H_2O)_2]Cl_2$	Green powder	18	296-294 °C	68
L^2Co	$[Co(L^3)(H_2O)_2]Cl_2$	Green powder	21	>300°C	66

Table 2. Physical properties of metal complexes.

Formula	DMSO	THF	DMF	acetone	chlorof	CH_2Cl_2	ethyl	hexane	acetoni	benzen	H_2O
$[Co(L^1)(H_2O)_2]Cl_2$	+	-	+	-	-	±	-	-	+	-	-
$[Co(L^2)(H_2O)_2]Cl_2$	+	-	+	-	-	±	+	-	+	-	-

Table 3. Solubility of prepared complexes.

+ = Slightly positive, - = Slightly positive

Com	ν_{C-H} Alph cm^{-1}	ν_{C-H} Arom cm^{-1}	$\nu_{HC=N}$ cm^{-1}	ν_{C-O} cm^{-1}	$\nu_{C=CAr}$ cm^{-1}	ν_{OH} cm^{-1}	ν_{M-H2O} cm^{-1}
L^1	2900m	3061w	1502s	1242s	1448s	3400m	------
L^2	2897m	3066vw	1643s	1224s	1463s	3458m	------
L^1Co	2902w	3044w	1604s	1261s	1455s	3150b	819m
L^2Co	2900w	3102w	1614s	1267s	1467s	3466b	808m

w = (weak) , m = (medium) , s = (strong) , b = (Broad)

Table 4. Characteristic IR bonds of the free ligands and its complexes.

ristic post complexation. A broadband (3200-3550 cm^{-1}) is present in all of the complexes, showing the presence of water molecules. Table (5) and Figures (7– 10) offer the ligands' UV–Visible spectral data and their complexes. At 225 nm and 246 nm, the aromatic band about the ligands L^1 and L^2, respectively, was seen to attribute to the vanillin π π* transition's phenyl. In these ligands, the azomethine group was seen as two bands because of the n π* and π π* transitions. In the complexes, these double bands were seen to shift to lengthier wavelengths. The spectra pertaining to the complexes (L^2Co) and (L^1Co) demonstrated two newer bands that had longer wavelengths (visible region), which were then assigned to the metal–ligand charge transfer (MLCT) bands and d–d transitions of the metal ion[12-14].

Com	(π–π*) phenyl (nm) Cycle	-C=N- (nm) (π—π *)	-C=N- (n–π*) (nm)	(C—T) (nm)	(d–d) (nm)
L^1	225	280	320	----	----
L^1Co	217	247	318	520	590
L^2	225	275	326	----	----
L^2Co	240	287	334	520	590

Table 5. Electronic spectral data for the free ligands and their complexes.

^1H, ^{13}C – NMR spectra of the ligands

Nuclear Magnetic Resonance (^{1}H-NMR) was used to characterize the ligands L^1 and L^2, which demonstrated that the ligands had various characteristic signals, as presented in Figures (11 – 12) and Table (6). The signs of OH and methyl groups (-CH_3) for L1 and L2 are observed in the 5.55 – 5.25 ppm and 3.80–2.4 ppm, respectively. The signals of aromatic protons are detected in the 7.3–6.0 ppm range. The signs at 8.5 – 7.75 ppm were attributed to the azomethine proton (-HC=N-). The ^{13}C – NMR data relating to the ligands corresponded with the ^{1}H – NMR data mentioned above, as presented in Figures (13– 14) and Table (7), thereby validating the put forward structure of the ligands[15].

General properties of complexes

The atomic absorption information, molecular weight, molar conductivity, and magnetic susceptibilities pertaining to the complexes are shown in Table (8). As seen via atomic absorption measurements, the reaction of ligands L^1 and L^2 with the Co (II) salt ions at a molar ratio of 1:1 yielded metal complexes. Rast's camphor method was employed to calculate the molar weight of the complexes (L^1Co) and (L^2Co), and as per the results, the practical data agreed with the suggested general formula pertaining to the complexes. Johns and Brad method were employed for measuring the molar conductivity related to the complexes by maintaining

Protons	δ (chemical shift ppm)	
Symbol	L^1	L^2
C_1	8.3	7.75
C_2	7.3	7.2
C_3	7.1	6.75
C_4	6.75	6.5
C_5	5.9	5.9
C_6	5.34	5.25
C_7	3.6	3.75
C_8	-----	2.4
C_9	-----	-----
C_{10}	-----	-----

Table 6. Chemical shift of ^{1}H-NMR for the ligands.

Protons	δ (chemical shift ppm)	
Symbol	L^1	L^2
C_1	160.08	160.8
C_2	149.69	149.69
C_3	148.23	148.23
C_4	131.17	143.88
C_5	130.57	138.13
C_6	124.17	134.17
C_7	108.37	132.58
C_8	106.93	131.17
C_9	102.12	128.87
C_{10}	61.27	127.17
C_{11}	-----	108.37
C_{12}	-----	106.93
C_{13}	-----	102.12
C_{14}	-----	61.27
C_{15}	-----	28.78

Table 7. Chemical shift of ^{13}C-NMR for the ligands.

Com.	Formula	M.wt Camphor Method		Molar conductivity $Ohm^{-1}.cm^{-1}/mol$	Metal %		M:L ratio	Atomic magnetic susceptibility $X_A.10^{-6}$	μeff (BM)
		found	Cal		found	Cal			
L^1Co	$[Co(L^1)(H_2O)_2]Cl_2$	482.5	483.07	219.32	11.17	11.32	1:1	2713.49	2.424
L^2Co	$[Co(L^3)(H_2O)_2]Cl_2$	500.02	498.10	198.18	12.02	11.98	1:1	2513.49	2.162

Table 8. Molar conductivity, molecular weight, magnetic measurements, and atomic absorption data of the complexes.

room temperature ($1x10^{-3}$ M) in DMF. The complexes had high molar conductance values, demonstrating that all the complexes acted as electrolytes because of chlorine ions present outside the coordination sphere. A chemical analysis was performed to confirm this result, wherein precipitate was yielded by the chloride ions when $AgNO_3$ solution was introduced. Faraday's method measured the magnetic moment (μ_{eff}) pertaining to the ligand complexes when maintained at room temperature. For complexes (L^1Co) and (L^2Co), the (μ_{eff}) values were found to be 2.424 and 1.521 BM, respectively, highlighting that a tetrahedral geometry was associated with the L^1Co complex. In contrast, a square planar geometry was related to the L^2Co complex[15-17].

Antibacterial activity of the ligands and complexes

Table 9 shows the values of the antibacterial activity to the Schiff base ligands as well as their complexes performed against gram-negative and gram-positive bacteria. It is observed from this work that L^1Co metal chelate has a lower activity when compared to the parent ligand against gram-positive bacteria and gram-negative bacteria. On the other hand, L^2Co metal chelate exhibits lower activity against gram-positive and gram-negative bacteria as compared to the original ligand. In the Schiff base ligands and complexes, the order pertaining to the antimicrobial activity was (L^1 L^2) and (L^2 L^1Co). This data is attributed to the fact that biological activity grows with growing molecular weight and distance between the azomethine groups[18,19].

Modeling and Geometrical Optimization

Quantum chemical calculations were performed for four compounds using the GAUSSIAN 03 program[20]. At the DFT/B3LYP level of theory, the analyses were carried out by employing the basis set B3LYP/6-31+G (d,p). Pentium (R) 4/IPM-PC- CPU 3.00GHz, 2.00GB was used to perform all calculations. Figure 1 displays the structures pertaining to the compounds. The geometries of the Schiff base ligands and Co complexes were optimized by employing the B3LYP function. With regards to the Cu atom, the LANL2DZ basis set was employed, while for all the non-metal atoms, the 6-31+G (d,p) basis set was employed[21,22]. Calculation of the frequency was done based on this optimised geometry to ensure that the global minima lacked an imaginary frequency. The optimised structures were employed to compute MESP and FMO. The Gaussian-09 program package was employed for all the calculations.

The key elements affecting molecular activity include frontier molecular orbitals, which also correspond to LUMO and HOMO orbitals. Table 10 shows the LUMO, HOMO and gap energies corresponding to the ligands as well as their complexes. An ongoing decrease in the LUMO levels was seen for the L^1 and L^2Co molecules, resulting in the reduced stability of L^1 and L^2, whereas the low HOMO energy of L^2 and its high LUMO energy led to an increase in their stability compared with the other compounds. L^1, with a high EHOMO value, had a lot of power to provide electrons to the unoccupied d orbital of the metal compared with L^2. Furthermore, L^1, with a low ELUMO value, had a high power to obtain electrons from the metal[23]. The global chemical reactivity properties, like the chemical potential (μ), chemical hardness (η) and electrophilicity (ω), were calculated based on the LUMO and HOMO energy values. Potential, which indicates the propensity to release electrons, can be expressed as $\mu = (E_{HOMO}+E_{LUMO})/2$[24,25]. Table 11 shows that L^2Co had a smaller electronic chemical potential than the other compounds. This indicated that these molecules were more stable since the electrons would not leave the system. Chemical hardness may be regarded as the resistance of molecules to the exchange of electrons with their surroundings. This can be represented as $\eta = (E_{LUMO} - E_{HOMO})/2$[26]

Compounds	Gram-positive bacteria	Gram-negative bacteria
DMSO	-	-
L^1	+++	++
L^2	++++	++++
L^1Co	++	+++
L^2Co	+++	++++

Inhibition zone diameter in mm (-) 0, (+)7-10, (++)10-15 (+++) 15-19, (++++) 19-20.

Table 9. Biological activity results of the ligands and complexes.

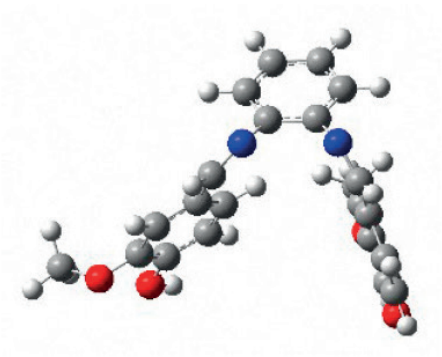

L^1

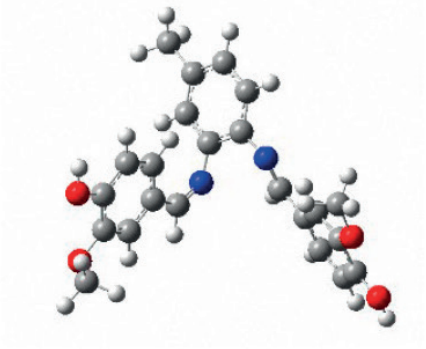

L^2

L^1Co

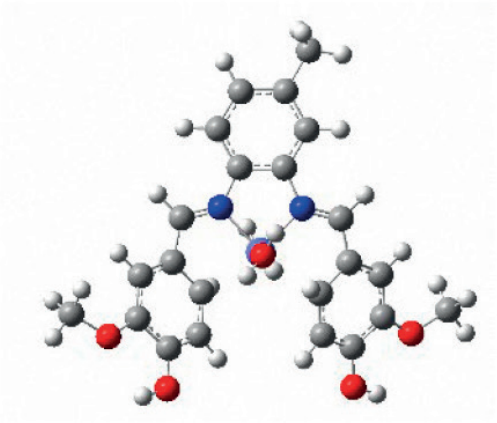

L^2Co

Figure 15. Optimised structures of L^1, L^2, L^1Co and L^2Co complexes according to DFT/ B3LYP/6-31+G (d,p) level of theory.

and pertain to the chemical system's reactivity as well as stability. A hard molecule is one that has a large HOMO-LUMO gap. A molecule with a large gap becomes more stable and requires a lot of excitation energy to reach the excited state regions[27]. L^2 had a high chemical hardness compared to the other compounds, as indicated in Table 11. As a result, L^2 had harder and less reactive molecules than the others. Electrophilicity (ω) measures the stability of a molecule when it gains extra electrons, and it is expressed as $\omega = \mu^2/2\eta$[26]. The electrophilicity decreased in the order L^2Co, L^1, L^2, and L^1Co. As a result, L^2Co appeared to be more stable and was hence, less reactive when accepting electrons .

Conclusions

The synthesis and characterization of the substances under research were disclosed in this paper. The square planar geometry of the Cu (II) complex was hypothesized based on the electronic spectrum data, conductance measurements, and the FTIR observations mentioned above. Following total optimization by B3LYP/6-31+G (d,p) for the ligand and LANL2DZ for the complexes, the quantum chemical investigation of the geometries and electronic properties of the ligand and complexes, optimized geometric structures, the HOMO, LUMO, as well as the energy band gap (E), has been investigated. From the results of the total optimized structures, it is noted that the energy gap of the ligand is larger than complexes. Energy gap for the compounds understudy are $L^2 > L^1Co > L^2Co > L^1$, because of the ligand L^2 have maximum hardness and high stability in relation to the values of hardness, energy gap while the compounds L^1 and L^2Co with a small hardness and energy gap this can be associated with a high chemical reactivity and low kinetic stability. For ligands and all complexes, the structure of the compound changes slightly. This results in a redistribution of the electron cloud in the compound, implying that different structures play a key role in the effects of electronic properties and subtle structural changes. For ligands and all complexes, the structure of the compound changes slightly. This leads to a redistribution of the electron cloud in the compound, which means that different structures play a key role in the effects of electronic properties and subtle structural changes, which prove it by DFT calculation. This calculation can be used as a model system to understand the relationship between electronic properties and molecular structure and can be used to study their applicability. The antibacterial activities of the prepared ligands and their complexes against Gram-negative and Gram-positive bacteria were also examined.

Supplementary Materials

Table 1: Some physical properties of prepared Schiff base ligands, Table 2: Solubility of prepared Schiff base ligands. Table 3: Physical properties of prepared complexes.

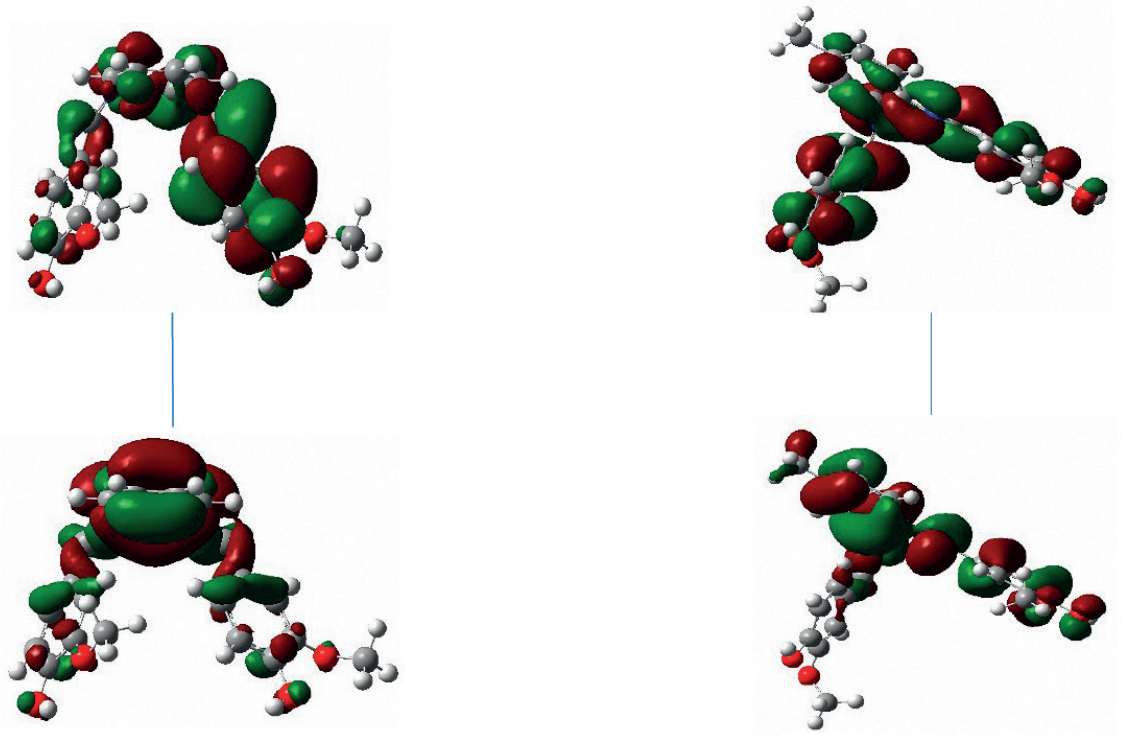

Figure 16. The frontier orbitals, HOMO and LUMO of calculated at the B3LYP/6-31+G (d,p) level of theory for ligand.

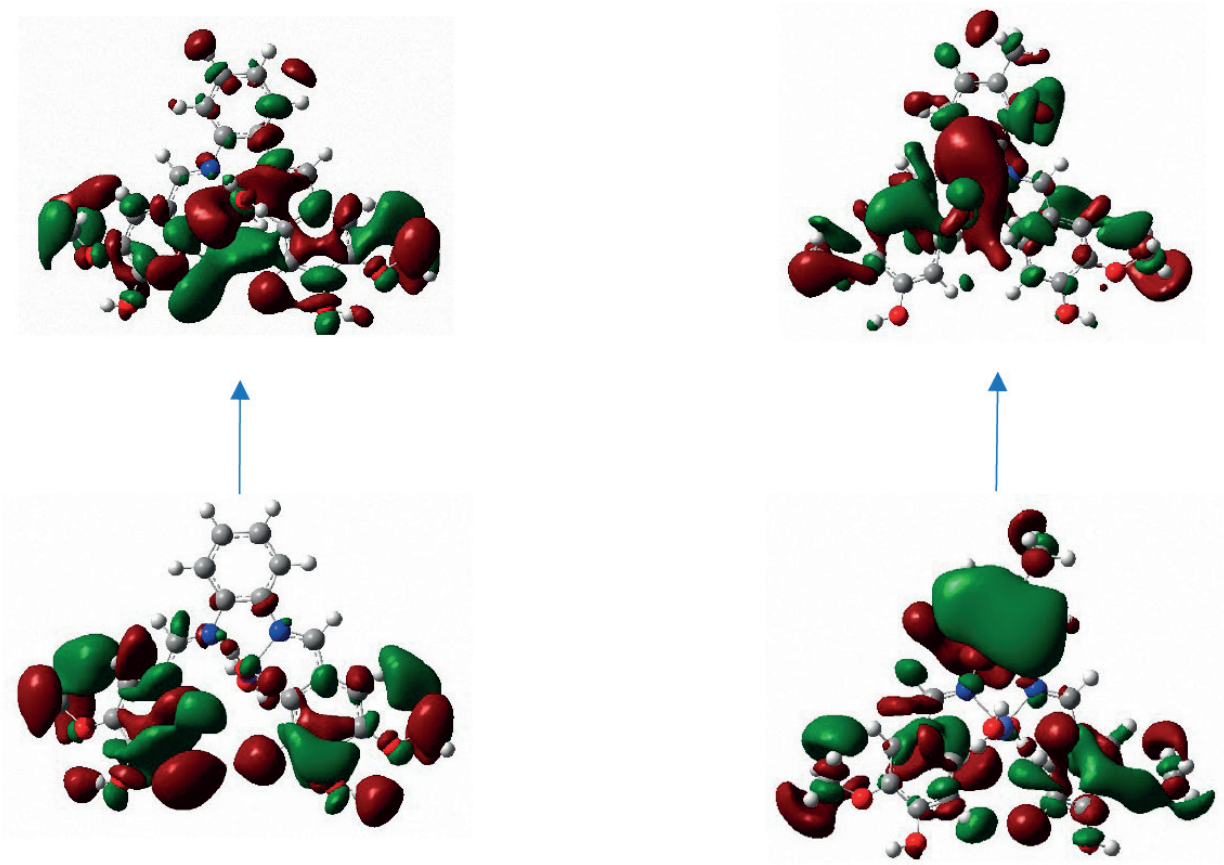

Figure 17. The frontier orbitals, HOMO and LUMO of calculated at the B3LYP/LANL2DZ level of theory for complexes.

Com	HOMO eV	LUMO eV	ΔE eV	ω	η	μ	S	X	A	I
L^1	-0.06911	0.02666	0.0957	0.0047	0.0478	-0.0212	20.8833	0.0212	-0.027	0.06911
L^2	-0.1414	0.1014	0.2429	0.00164	0.1214	-0.02	8.2372	0.02	-0.101	0.1414
L^1Co	-0.1164	0.09415	0.21061	0.000587	0.1052	-0.01113	9.4989	0.01113	-0.094	0.21055
L^2Co	-0.1213	0.0288	0.15020	0.01425	0.0750	-0.04625	13.3244	0.04625	-0.029	0.1213

HOMO= *The energy of Highest Occupied Molecular Orbital,* **LUMO=** *The energy of Lowest Unoccupied Molecular Orbital,* (Δ*E*)=energy band gap, **ω=** *Electrophilicity index,* **η=** Global hardness, **μ=** *Chemical potential,* ***S***=Softness, ***X***= Electronegative, **A=** Electronaffinity, **I=** Ionizationpotential.

Table 10. Ground state properties of the ligand and its metal complexes using B3LYP/6-31+G (d,p) for its complexes and B3LYP/LANL2DZ.

Table 4: Solubility of prepared complexes. Table 5: Characteristic IR bonds of the ligands and the complexes. Table 6: Electronic spectral data for the ligands and their complexes. Table 7: Chemical shift of ^{1}H-NMR for the ligands. Table 8: Chemical shift of ^{13}C-NMR for the ligands. Table 9: Molecular weight, molar conductivity, magnetic measurements and atomic absorption data of the complexes. Table 10: Biological activity data of the ligand and complex. Table 11. Ground state properties of the ligand and its metal complexes using B3LYP/6-31+G (d,p) for the ligand and B3LYP/LANL2DZ for its complexes.

Figure 1: Chemical structure of the prepared Schiff base ligands. Figure 2: Structure of the prepared complexes. Figure 3: I.R Spectrum of the ligand (L^1). Figure 4: I.R Spectrum of the ligand (L^2). Figure 5: I.R Spectrum of the ligand L1Co. Figure 6: I.R Spectrum of the complex (L^2Co). Figure 7: UV spectrum of the ligand (L^1).

Author Contributions

Conceptualization, methodology, validation, formal analysis, resources, writing original draft, and review and editing, A M and J M, data curation, visualization, S M-H, formal analysis, Software, project administration k A. All authors have read and agreed to the published version of the manuscript." Please turn to the CRediT taxonomy for the term explanation. Authorship must be limited to those who have contributed substantially to the work reported.

Funding

This research received no external funding.

Conflicts of Interest

The authors declare no conflict of interest.

Bibliographic references

1. Puchtler, H.; Meloan, S. N.; On Schiff's Bases and Aldehyde-Fuchsin: A Review from H. Schiff to R.D. Lillie., Histochemistry, 1981, 72, pp.321-332.
2. Jessica, C.; Domenico, I.; Alessia. C.; Francesca, C.; Rosamaria, L and Maria, S. S. A Review on the Antimicrobial Activity of Schiff Bases: Data Collection and Recent Studies, Antibiotics, 2022, 11, 191. DOI: org/10.3390/antibiotics11020191.
3. Manzoor, A. M.; Shabir, A. L.; Parveez, G.; Ovas, A. D.; Mohmmad, Y. W.; Aijaz, A and Athar, A. H. Efficacy of Novel Schiff base Derivatives as Antifungal Compounds in Combination with Approved Drugs Against Candida Albicans, Medicinal Chemistry, 2019, 15, 1-11. DOI: 10.2174/1573406415666181203115957.
4. Thamer, A. A.; Ahmed, N. Al-H.; Saeed, S, E S.; Ebtesam, H. L. A.; Abuzar E.A.E. A. Synthesis, characterization, and anticancer activity of some metal complexes with a new Schiff base ligand, Arabian Journal of Chemistry, 2022, 15, 2, 103559., DOI: org/10.1016/j.arabjc.2021.103559.
5. Cristina, I. F.; Pedro, D. Vaz.; Teresa, G, N.; Carla, D, N. Zinc biomimetic catalysts for epoxidation of olefins with H2O2., Applied Clay Science., 2020, 190, 105562., DOI: org/10.1016/j.clay.2020.105562.
6. Hongzhi, D.; Xuan, P.; Haiyang, Yu.; Xiuli, Z.; Xuesi, C.; Dongmei, C.; Xianhong, W and Xiabin, J.; Polymerization of rac-Lactide Using Schiff Base Aluminum Catalysts: Structure, Activity, and Stereoselectivity., Macromolecules, 2007, 40, 1904-1913.
7. Anna, L.; yutang, L and Kenneth, W, Catalysts, 2020, 10, 705; DOI:10.3390/catal10060705.
8. Victor, I. M.; Denis, A. C.; Lidiya, V. Y.; Nikolai, S. I.; Michail, M. I. Asymmetric ring opening of epoxides with cyanides catalysed by chiral binuclear titanium complexes., Tetrahedron: Asymmetry, 2014, 25, 838–843. DOI: org/10.1016/j.tetasy.2014.04.
9. Basim, H. A.; Mohammed, M. H.; Ahmad, H, I.; New complexes of chelating Schiff base: Synthesis, spectral investigation, antimicrobial, and thermal behavior studies, Journal of Applied Pharmaceutical Science, 2019, 9 (04), 045-057. DOI: 10.7324/JAPS.2019.90406.
10. Hassan, W. G.; Muhammad, S. A.; Mohamad, S. S. J and Nor, A. Endot. Efficient Catalytic Reduction of 4-Nitrophenol Using Copper(II) Complexes with N,O-Chelating Schiff Base Ligands, Molecules, 2021, 26, 5876. DOI: org/10.3390/ molecules, 26195876.
11. Lamia, S. A.; Ibtisam, K. M.; Rehab, K. R. A. A review on versatile applications of transition metal complexes incorporating schiff bases from amoxicillin and cephalexin, EurAsian Journal of BioSciences, 2020, 14, 7541-7550.
12. Linda, B.; Jan, R.; Vaclav, E.; Amel, I.; Monia, E and Rached, B. H. Crystal Structure, Hirshfeld Surface Analysis and Biological Activities of trans-Dipyridinebis (3-Acetyl-2-Oxo-2H-Chromen-4-Olato)Cobalt(II), Acta Chim. Slov. 2019, 66, 603–613. DOI: 10.17344/acsi.2019.5002.

13. Athmar, A. K.; Ibtihal, K. K.; Abid, A. M. A.; Synthesis and Spectral Identification of New Azo-Schiff Base Ligand Derivative from Aminobenzylamine and its Novel Metal Complexes with Cu(II), Zn(II) and Hg(II), International Journal of Drug Delivery Technology. 2022, 12(1):150-156. DOI: 10.25258/ijddt.12.1.27.
14. Ali, Ç.; Gökhan, C.; Mehmet, S.; Synthesis, characterization and catalytic properties of some transition metal complexes of new phenoxy-imine ligand, Int. J. Chem. Technol. 2017, 1, 37-45.
15. Zainab, A. M. S.; Mariam, A. A and Abduljlee, M., Synthesis, Characterization and Thermal Studies of Schiff Bases derived from 2-Pyridinecarboxaldehyde and Benzaldehyde and their Complexes with Cupper (II) and Cobalt (II), Der Pharma Chemica, 2016, 8 (20):85-96.
16. Imran, A.; Waseem, A. Wani and Kishwar, S.; Empirical Formulae to Molecular Structures of Metal Complexes by Molar Conductance., Synthesis and Reactivity in Inorganic, Metal-Organic, and Nano-Metal Chemistry , 2013, 43:1162–1170, DOI: 10.1080/15533174.2012.756898.
17. Sultanaa, U. S.; Habib, M. A.; Md, K. A,; Md, M.; Md, K and Nazmul Islama A.B.Mm.; Synthesis, Structural Properties of Hydrazine Carbodithioate Schiff Base and Their Metal Complexes and Evaluation of Their Biological Activity, Egypt. J. Chem.2022, 63, 10, pp. 3811 – 3816. DOI: 10.21608/ejchem.2020. 20507.2230.
18. Chamidah, A., H and Prihanto, A. A., Antibacterial Activities of β-Glucan (Laminaran) against Gram-Negative and Gram-Positive Bacteria, Antibacterial activities of β-glucan (laminaran) against gram-negative and gram-positive bacteria, AIP Conference Proceedings, 2017, 1844, 020011. DOI: org/10.1063/1.4983422.
19. Lourdes, Ortego.; Jesús, G-A.; Antonio, L.; Villacampa, M. D.; Gimeno, M. C, (Aminophosphane)gold(I) and silver(I) complexes as antibacterial agents, Journal of Inorganic Biochemistry, 2015, 19-27, DOI: org/10.1016/j.jinorgbio.2015.01.007.
20. Frisch M J. Trucks G W. Schlegel H B. Scuseria G E. Robb M A. Cheeseman J R. Scalmani G. Barone V. Mennucci B. Petersson G A. Nakatsuji H. Caricato M. Li X. Hratchian H P. Izmaylov A F. Bloino J. Zheng G. Sonnenberg J L. Hada M. Ehara M. Toyota K. Fukuda R. Hasegawa J. Ishida M. Nakajima T. Honda Y. Kitao O. Nakai H. Vreven T. Montgomery J J A. Peralta J E. Ogliaro F. Bearpark M. Heyd J J. Brothers E. Kudin K N. Staroverov V N. Kobayashi R. Normand J. Raghavachari K. Rendell A. Burant J C. Iyengar S S. Tomasi J. Cossi M. Rega N. Millam J M. Klene M. Knox J E. Cross J B. Bakken V. Adamo C. Jaramillo J. Gomperts R. Stratmann R E. Yazyev O. Austin A J. Cammi R. Pomelli C. Ochterski J W. Martin R L. Morokuma K. Zakrzewski V G. Voth G A. Salvador P. Dannenberg J J. Dapprich S. Daniels A D. Farkas O. Foresman J B. Ortiz J V. Cioslowski J. Fox D. J. Gaussian 09, Revision A. 1. Gaussian, Inc., Wallingford, 2009.
21. Sarah K. Alessandro P. Henk B. Michele S. Giulia L. Laura M. José M J. Edwin C C. Enrique O and Catherine E H. Luminescent copper(I) complexes with bisphosphane and halogen-substituted 2,2'-bipyridine ligands. J. Name., 2013, 00, 1-3. DOI: 10.1039/x0xx00000x.
22. Niaz M. Mukhtar A. Muhammad S. Zafar A. Nikolay T. Johan W. Abdelbasset C. Kübra S. Ahmet M. Shabbir M. Shaukat S. Saqib A and Abdullah G A. Synthesis, Characterization,Biological Activity and Molecular Docking Studies of Novel Organotin(IV) Carboxylates. Frontiers in Pharmacology, 2022, 13, DOI: org/10.3389/fphar.2022.864336.
23. Loutfy H M. Elroby S K. Inhibitive properties, thermodynamic, kinetics and quantum chemical calculations of polydentate Schiff base compounds as corrosion inhibitors for iron in acidic and alkaline media. Int J Ind Chem, 2015, 6:165–184. DOI:10.1007/s40090-015-0039-7.
24. Ummi L M R. Karimah K. Amalina M T. Muhamad K Y and Nurul A Z. Synthesis, Characterization, DFT and Antibacterial Screening of Schiff Base Derived from Isatin with Thiocarbohydrazide and Their Cu(II) And Zn(II) Complexes. Malaysian Journal of Chemistry, 2022, 24(2), 250-257.
25. Hilaire T. Stanley N. Didier A F T. Fritzgerald K B and Julius N G. Theoretical Study of the Structural, Optoelectronic, and Reactivity Properties of N-[59-Methyl-39-Isoxasolyl]-N-[(E)-1-(-2-)]Methylidene] Amine and Some of Its Fe2+, Co2+, Ni2+, Cu2+, and Zn2+ Complexes for OLED and OFET Applications. Journal of Chemistry, 2022, ID 3528170, 18. DOI: org/10.1155/2022/3528170.
26. Luis R D. Mar R and Patricia P. Applications of the Conceptual Density Functional Theory Indices to Organic Chemistry Reactivity Molecules, 2016, 21, 748; DOI:10.3390/molecules21060748.
27. Md J. Md J A. Md K H. Mohammad A H. Ullah O U. Molecular docking and dynamics of Nickel-Schiff base complexes for inhibiting β-lactamase of Mycobacterium tuberculosis, In Silico Pharmacology. 2018, 6,6, DOI: 10.1007/s40203-018-0044-6.
28. Walid L. Salima B. Lorraine C. Christophe M and Henry C. Coordination Chemistry of Zn2+ With Sal(ph)en Ligands: Tetrahedral Coordination or Penta-Coordination? A DFT Analysis. J. Comput. Chem. 2019, 40, 717–725, DOI:10.1002/jcc.25755.